

This article was downloaded by:

On: 14 January 2011

Access details: *Access Details: Free Access*

Publisher *Taylor & Francis*

Informa Ltd Registered in England and Wales Registered Number: 1072954 Registered office: Mortimer House, 37-41 Mortimer Street, London W1T 3JH, UK



Molecular Simulation

Publication details, including instructions for authors and subscription information:

<http://www.informaworld.com/smpp/title~content=t713644482>

3D-QSAR method on indole and pyrrole inhibitors of monoamine oxidase type A

Younho Lee^a; Yoongho Lim^a

^a Division of Bioscience and Biotechnology, BMIC, RCD, Konkuk University, Seoul, South Korea

To cite this Article Lee, Younho and Lim, Yoongho(2009) '3D-QSAR method on indole and pyrrole inhibitors of monoamine oxidase type A', *Molecular Simulation*, 35: 15, 1242 – 1248

To link to this Article: DOI: 10.1080/08927020902974055

URL: <http://dx.doi.org/10.1080/08927020902974055>

PLEASE SCROLL DOWN FOR ARTICLE

Full terms and conditions of use: <http://www.informaworld.com/terms-and-conditions-of-access.pdf>

This article may be used for research, teaching and private study purposes. Any substantial or systematic reproduction, re-distribution, re-selling, loan or sub-licensing, systematic supply or distribution in any form to anyone is expressly forbidden.

The publisher does not give any warranty express or implied or make any representation that the contents will be complete or accurate or up to date. The accuracy of any instructions, formulae and drug doses should be independently verified with primary sources. The publisher shall not be liable for any loss, actions, claims, proceedings, demand or costs or damages whatsoever or howsoever caused arising directly or indirectly in connection with or arising out of the use of this material.

3D-QSAR method on indole and pyrrole inhibitors of monoamine oxidase type A

Younho Lee¹ and Yoongho Lim*

Division of Bioscience and Biotechnology, BMIC, RCD, Konkuk University, Hwayang-Dong 1, Gwangjin-Ku, Seoul 143-701, South Korea

(Received 15 October 2008; final version received 9 April 2009)

Monoamine oxidase A (MAO-A) converts norepinephrine and serotonin to an oxidative form. These monoamine neurotransmitters have important roles in depression. The MAO-A inhibitors have been discovered for neurodegenerative disease therapy. In order to design novel MAO-A inhibitors, in this study, the quantitative structure-activity relationships for the combined series of indoles and pyrroles were elucidated and the structural conditions to show good inhibitory effects on MAO-A were derived. This result can help us design new inhibitors irrespective of their specific moiety.

Keywords: monoamine oxidase A; quantitative structure-activity relationships; indole; pyrrole

1. Introduction

The drug market targeting the central nervous system (CNS) increased dramatically by 70 billion dollars in 2005, the fastest growing rate except for cardiovascular drugs. Among CNS drugs, anti-depressants occupy 23% of the drug market and, therefore, many anti-depressants have been researched and developed. One of the oldest classes of anti-depressants is an inhibitor of monoamine oxidase (MAO). MAO is a flavoenzyme and is divided into two isoforms, type A and type B. MAO-B prefers dopamine and beta-phenylethylamine as its substrate [1]. Inhibitors of MAO-B have been studied for both Parkinson's disease and Alzheimer's disease. MAO-A converts norepinephrine and serotonin to an oxidative form. These monoamine neurotransmitters have important roles in depression [2,3]. The X-ray crystallographic structure of the human MAO-A was released in 2005 and the rat MAO-A structure in 2004 [4]. The human MAO-A contains 527 amino acids which are composed of flavin-adenine dinucleotide (FAD)-binding domain, the substrate-binding domain and the C-terminal membrane region. The inhibitory selectivity of MAO-A and MAO-B is caused by the structural differences between Ile-335 of MAO-A and Tyr-326 of MAO-B [4]. The X-ray crystallographic structure of MAO-A can help us predict good ligands using *in silico* computational methods. MAO inhibitors (MAOIs) have been discovered during the last five decades for use in neurodegenerative disease therapy. The first generation of MAOIs was irreversible and non-selective resulting in severe side effects like hypertensive crisis [5,6]. To overcome these problems, the next generation of reversible and

selective MAOIs was developed, such as moclobemide and toloxatone, which were used as anti-depressants and anxiety treatment drugs. Since these too had side effects, such as bone marrow damage and increase in anxiety, there have been renewed efforts towards the discovery of new MAO-A inhibitors. In this study, to design novel MAO-A inhibitors, computational tools were introduced.

2. Materials and methods

The compounds used for the quantitative structure–activity relationships (QSAR) with three dimensional-comparative molecular field analysis (CoMFA) were obtained from the papers published previously by Morón, Silvestri, Santo and Regina [7–10]. They included 96 compounds showing the inhibitory activities against MAOs. Of them, only 34 compounds were selected based on the selectivities between MAO-A and MAO-B as 5-fold and the kinetic constants of the competitive inhibition ($K_i < 18 \mu\text{M}$). The activities of the compounds in the four papers were standardised by comparing them with the activity of clorgyline used as a reference in each paper. The K_i values of indole derivatives had been optimised by multiplying 1.8-fold because the K_i value of the reference compound, clorgyline was 1.8-fold lower than those of the experimental data of pyrrole derivatives [11].

The 3D structures of 34 compounds were built up using an Intel Core 2 Quad Q6600 (2.4 GHz) Linux PC with Sybyl 7.3 (Tripos, St Louis, MO, USA). The compounds were subjected to energy minimisation. The minimisation process was ceased at the convergence

*Corresponding author. Email: yoongho@konkuk.ac.kr

Table 1. The structures of the compounds used for QSAR and their biological data which are expressed in negative log scale of the kinetic constants of the competitive inhibition ($K_i/\mu\text{M}$).

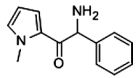
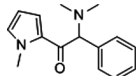
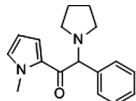
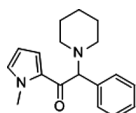
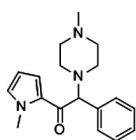
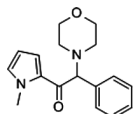
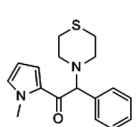
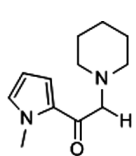
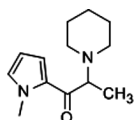
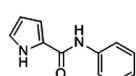
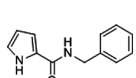
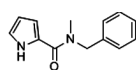
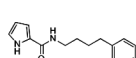
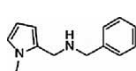
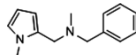
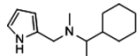
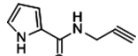
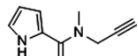
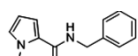
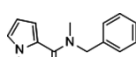
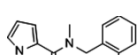
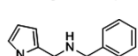
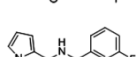
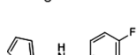
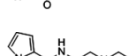
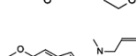

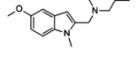
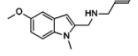
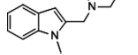
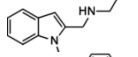
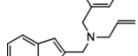
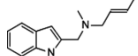
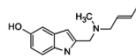
Compound number	Structure	Experimental pK _i .	Predicted pK _i .	Residuals
1 [9]		1.02	1.108	-0.088
2 [9]		-0.24	1.402	-1.642
3 [9]		2.12	2.021	0.099
4 [9]		1.02	1.149	-0.129
5 [9]		0.46	0.537	-0.077
6 [9]		0.46	0.472	-0.012
7 [9]		1.00	0.796	0.204
8 [9]		2.15	2.136	0.014
9 [9]		1.42	1.505	-0.085
10 [9]		0.4	0.325	0.075
11 [8,10]		0.6	0.551	0.049
12 [8,10]		0.22	0.212	0.008
13 [10]		1.26	1.226	0.034
14 [10]		1.62	1.612	0.008
15 [10]		0.82	0.849	-0.029

Table 1 – continued

Compound number	Structure	Experimental pKi.	Predicted pKi.	Residuals
16 [10]		1.70	1.694	0.006
17 [10]		0.64	0.665	– 0.025
18 [8,10]		1.12	1.052	0.068
19 [8]		0.59	0.671	– 0.081
20 [8]		0.27	0.354	– 0.084
21 [8]		0.74	0.718	0.022
22 [8]		0.40	0.353	0.047
23 [8]		0.47	0.362	0.108
24 [8]		0.14	0.320	– 0.18
25 [8]		0.40	0.367	0.033
26 [7]		2.57	2.496	0.074
27 [7]		2.60	2.490	0.11
28 [7]		2.84	2.935	– 0.095
29 [7]		3.27	3.339	– 0.069
30 [7]		0.36	3.240	– 2.880
31 [7]		– 1.25	2.231	– 3.481
32 [7]		2.11	2.070	0.04
33 [7]		1.99	2.101	– 0.111
34 [7]		2.14	2.083	0.057

Of 34 compounds, 29 compounds (except **8**, **14**, **22**, **27**, **34**) were selected for the training set and others were used for the test set. The 4th column lists the predicted values obtained by the QSAR calculations. The 5th column shows the differences between the experimental values and the predicted values. The superscripts on the compound numbers denote the reference numbers which the compounds were quoted from.

criteria of the total energy (0.05 kcal/molÅ). The 3D-QSAR was carried out using a Sybyl 7.3 program. All compounds were aligned with a DATABASE Alignment module provided by the Sybyl program. The substituents of pyrrole derivatives can be placed far from the FAD-binding domain or close, so that two different alignments were performed.

The partial least-square analysis was carried out to obtain the correlation between the biological activities and descriptors showing the physicochemical properties of the compounds. In order to get a linear scale, the values of the biological activities (K_i) were expressed in the negative log scale (pKi). Consequently, pKi values were used for the QSAR calculations. The cross-validation analysis was performed using the 'leave one out' (LOO) method. The optimum number of components obtained from the LOO method was applied to derive the final non-cross validated correlation r^2 . The best CoMFA model was improved by region focusing method. To check the CoMFA model, the activities of the compounds contained in the training set were predicted and compared with the experimental data.

For the docking study, two X-ray crystallographic structures containing the inhibitors clorgyline (2BXR.pdb) and harmine (2Z5X.pdb) were used. The docking experiments were performed on an Intel Pentium D CPU 2.80 GHz Linux PC with Insight 2005 (Accelrys, San Diego, CA, USA).

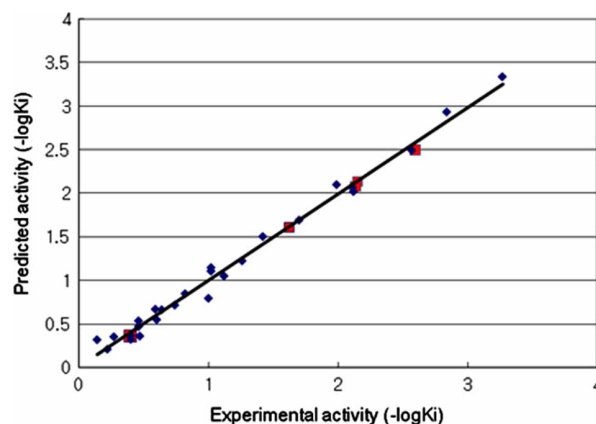


Figure 1. The correlation of the experimental values plotted against the predicted values obtained by QSAR. The blue diamond indicates the training set and the red square, the test set.

3. Results and discussion

A data set of 34 indole and pyrrole derivatives showing the inhibitory effects against MAO-A was selected for QSAR and docking studies (Table 1) [7–10].

The data set was split up into two groups such as a training set of 29 compounds to create QSAR models and a test set of 5 compounds (**8**, **14**, **22**, **27**, **34** in Table 1) to validate the models. All calculations were carried out on a

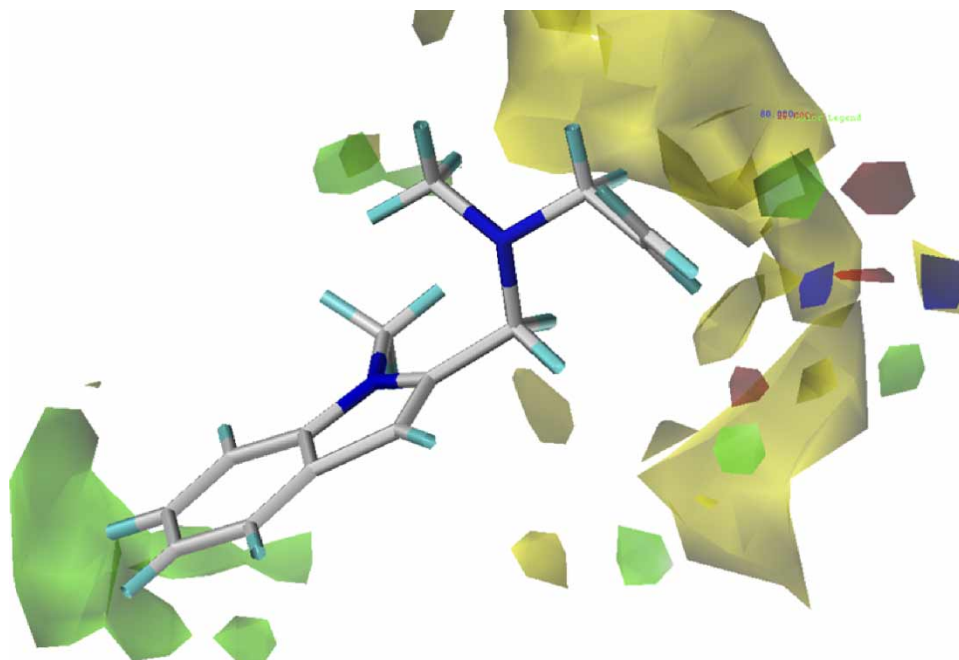


Figure 2. CoMFA contour maps with compound **29**. Green: steric bulk-favoured region, yellow: steric bulk-disfavoured region, blue: positive charge and hydrogen bond donor-favoured region, red: negative charge and hydrogen bond acceptors-favoured region. L1: the outside of the six-membered ring of indole, L2: the linear region, and L3: the electrostatic region.

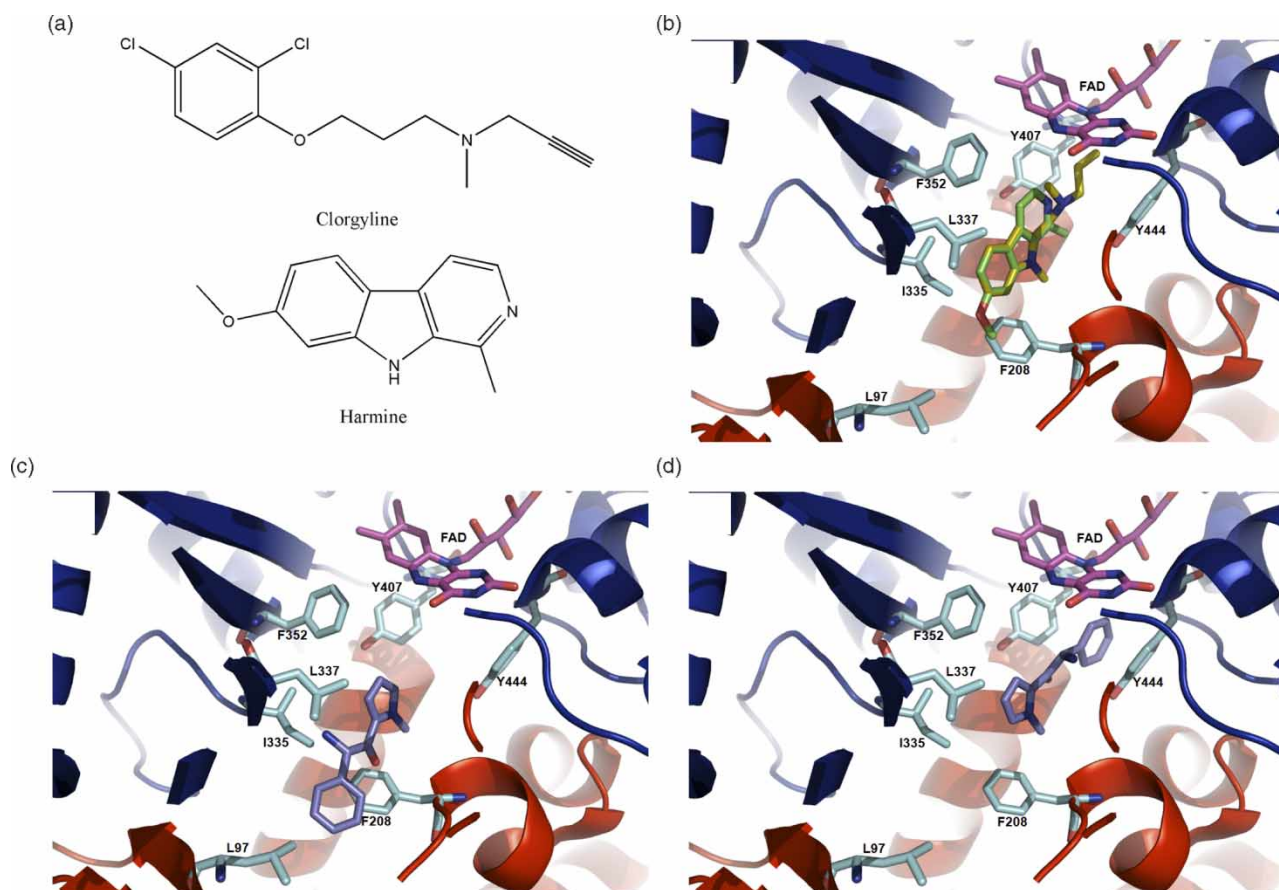


Figure 3. (a) The structures of clorgyline and harmine. (b) The substrate-binding site of the complex of MAO-A and harmine (2Z5X.pdb). The yellow coloured molecule denotes compound **29**, and green colour, harmine. (c) The substrate binding site of 2Z5X.pdb where compound **1** is docked. The pyrrole ring is placed from flavin-adenine dinucleotide (FAD) binding-domain. The blue coloured molecule denotes compound **1**. (d) The substrate-binding site of 2Z5X.pdb where pyrrole ring of compound **1** (blue) is placed close to FAD binding-domain.

Linux workstation PC with Sybyl 7.3 (Tripos, St Louis, MO, USA). A training set was used for CoMFA. Compounds **2**, **30** and **31** in Table 1 were outliers. Where these compounds were contained in the calculation, the QSAR model gave a lower value of the regression coefficient (r^2) than 0.5. Of the several models generated from CoMFA, the model showing the best cross-validated value (q^2) and the regression coefficient (r^2) was chosen, whose values were 0.870 and 0.991, respectively. The experimental values of the inhibitory activities obtained from the previous results [7–10] and the predicted values calculated by QSAR are listed in Table 1. The residual values between the experimental and predicted values are ranged between 0.006 and 0.204. To validate the QSAR model, a test set was selected. As listed in Table 1, the residual values between the experimental and predicted values for the test set are ranged within 0.110. Figure 1 shows the experimental values vs. the predicted values for the training set and the test set.

In order to visualise the relationships between the structures and their activities, CoMFA contour maps were obtained using Sybyl 7.3 program. The steric contribution and the electrostatic contribution are depicted in Figure 2. The corresponding field contributions of steric and electrostatic are 87 and 13%, respectively.

Compound **29** contains 'indole-methylamine' and its experimental value is the best among all the compounds in this experiment. It is displayed in the contour map. When the biological data of the compounds used in this experiment are observed, most indole derivatives show better activities than pyrrole derivatives. It can be expected that the benzene ring of indole contributes towards the activities. As expected, the green contour denoting the steric bulk-favoured region is observed around the benzene ring of indole. The opposite site of the indole group is surrounded by the yellow contour, so that the site is defined as steric bulk-disfavoured region. The electrostatic contours are observed in the region of heterocyclic ring involved in pyrrole derivatives such as compounds **5**, **6** and **7**.

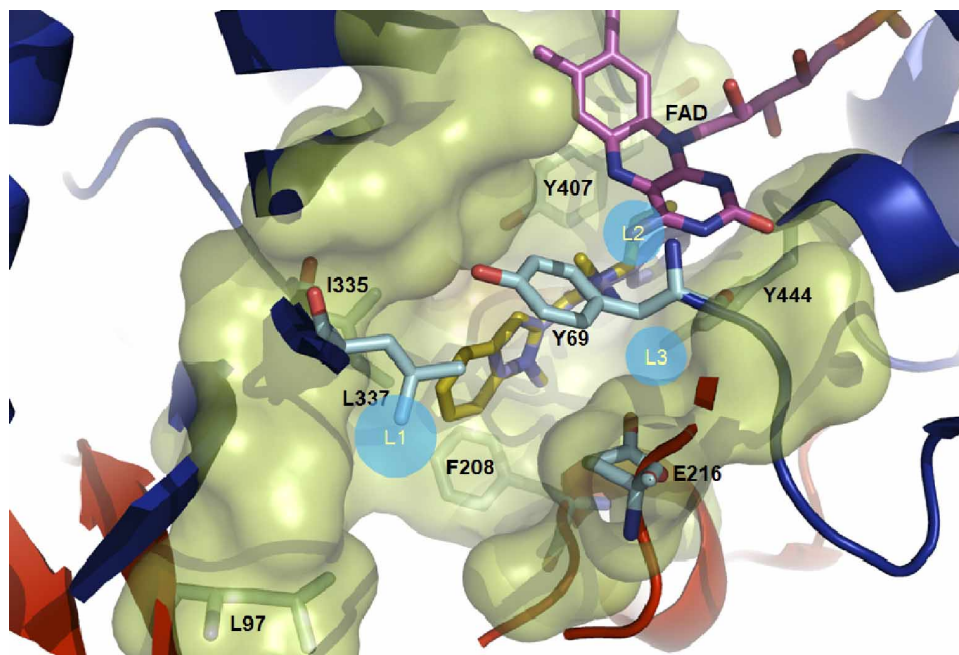


Figure 4. The region L1 contains the pyrrole or indole moiety, which is surrounded with L97, F208, I335 and L337. The region L2 contains the methylamine group, which consists of a cleft surrounded by Y407, Y444 and the FAD binding-domain. The electrostatic region L3 contains the heterocyclic ring which is close to E216. Compound **1** (blue) and compound **29** (yellow) are docked into the binding site.

In order to know the relationship between the contour maps of CoMFA and the active site of MAO-A, compounds **1** and **29** were selected as the representatives of pyrrole and indole derivatives, respectively. Most pyrrole derivatives used in this experiment contain the common features such as methyl group, benzene ring and amine group. Of them, compound **1** has a methyl group and a benzene ring, as well as a small amine group, so that it was chosen. For the superposition of the contour map and the active site, the docking models of the compound **1** and **29** were generated. Two MAO-A inhibitors, clorgyline (2BXR.pdb) and harmine (2Z5X.pdb), form the complex with MAO-A. The indole group of compound **29** is similar to harmine, and the methylamine group of compound **29** to clorgyline (Figure 3(a)).

The 2Z5X.pdb is the crystallographic structure of the complex of MAO-A, FAD, with harmine. When compound **29** was docked into the active site of MAO-A, the two ligands, harmine and compound **29**, superimposed well as shown in Figure 3(b). The indole groups of both ligands are placed far from the FAD-binding domain which includes about 20 residues. Of them, G66, G67, A68, Y69 and M445 enclosed flavin. The contour map obtained from CoMFA fits into the known active site of MAO-A. A similar experiment was carried out on clorgyline and compound **29**, and the same result was obtained. There is a pyrrole group present in compound **1**. Since indole contains a pyrrole ring, compound **1** was

docked into 2Z5X.pdb which has harmine. There are two possible conformations because two orientations of compound **1** are possible. Substituents of pyrrole derivatives are placed far from the FAD-binding domain or close (Figure 3(c) and (d)). Based on the interpretation of QSAR data, when substituents of pyrrole are close to the FAD-binding domain, they show better activities. The results agree with the known data published previously by Morón et al. [7] and Regina et al. [10].

The docking model obtained from compounds **1** and **29** described above was compared to the CoMFA contour map obtained from QSAR calculation. The region (L1) containing the pyrrole or indole moiety in the contour map favours bulky substituents. The corresponding position of the active site of MAO-A has a large cavity surrounded with L97, F208, I335 and L337 as shown in Figure 4.

Another region (L2) containing the methylamine group in the contour map favours non-bulky substituents. Its corresponding position in the active site of MAO-A contains Y407, Y444 and the FAD-binding domain, which consists of a cleft (Figure 4). In the case of harmine, the distance between the nitrogen of pyridine of harmine and the ketone of pyrimidine of FAD is about 4 Å. Because harmine consists of tricyclic rings, if a branch of the ligand is positioned to FAD, there can be a conflict. As a result, the region L2 does not like a bulky group. The electrostatic region (L3) of the contour map containing the heterocyclic ring is close to E216 of the active site in 2BXR.pdb

(Figure 4). While L1 and L2 regions are hydrophobic, L3 region is amphiphatic. In the active site of MAO-A, L1 and L2 regions are surrounded by L97, F208, I335, L337, Y407 and Y444, and L3 region, by Y69, E216 and Y444.

Based on the results obtained from the QSAR calculations and the docking study, for MAO-A inhibitors to show good inhibitory activities, their structural conditions are as follows: L1 region consists of a bulky-hydrophobic group. L2 region has a linear group. L3 region prefers a cyclic ring or heterocyclic ring. Many research groups evaluated various compounds as MAO-A inhibitors. For example, Chimenti et al. reviewed pyrazole derivatives [12], and Gallardo-Godoy et al. evaluated phenethylamines [13]. In addition, many results about each of the indole derivatives and pyrrole derivatives have been reported. In this study, the QSAR calculations for the combined series of indoles and pyrroles were tried and the structural conditions to show good inhibitory effects on MAO-A were derived. This result can help us design new inhibitors irrespective of their specific moiety.

Acknowledgements

This work was supported by the grants from the Korea Science and Engineering Foundation (No. M110751050004-07N5105-00410), Biogreen 21 (RDA), Agenda 11-30-68 (NIAS) and KRF-2006-005-J03402 (KRF).

Note

1. Email: zz265zz@konkuk.ac.kr

References

- [1] M.J. Kumar, D.G. Nicholls, and J.K. Andersen, *Oxidative α -ketoglutarate dehydrogenase inhibition via subtle elevations in monoamine oxidase B levels results in loss of spare respiratory capacity. Implications for Parkinson's disease*, J. Biol. Chem. 278 (2003), pp. 46432–46439.
- [2] A.M. Cesura and A. Pletscher, *The new generation of monoamine oxidase inhibitors*, Prog. Drug Res. 38 (1992), pp. 171–175.
- [3] M. Strolin-Benedetti and P.L. Dostert, *Monoamine oxidase: from physiology and patophysiology to the design and clinical applications of reversible inhibitors*, Adv. Drug Res. 23 (1992), pp. 65–125.
- [4] L.D. Colibus, M. Li, C. Binda, A. Lustig, D.E. Edmondson, and A. Mattevi, *Three-dimensional structure of human monoamine oxidase A (MAO A): relation to the structures of rat MAO A and human MAO B*, Proc. Natl. Acad. Sci. USA 102 (2005), pp. 12684–12689.
- [5] D.E. Edmondson, C. Binda, and A. Mattevi, *Structural insights into the mechanism of amine oxidation by monoamine oxidases A and B*, Arch. Biochem. Biophys. 464 (2007), pp. 269–276.
- [6] M. Yamada and H. Yasuhara, *Clinical pharmacology of MAO inhibitors: safety and future*, Neurotoxicology 25 (2004), pp. 215–221.
- [7] J.A. Morón, M. Campillo, V. Perez, M. Unzeta, and L. Pardo, *Molecular determinants of MAO selectivity in a series of indolylmethylamine derivatives: biological activities, 3D-QSAR/CoMFA analysis, and computational simulation of ligand recognition*, J. Med. Chem. 43 (2000), pp. 1684–1691.
- [8] R. Silvestri, G.L. Regina, G.D. Martino, M. Artico, O. Befani, M. Palumbo, E. Agostinelli, and P. Turini, *Simple, potent, and selective pyrrole inhibitors of monoamine oxidase types A and B*, J. Med. Chem. 46 (2003), pp. 917–920.
- [9] R.D. Santo, R. Costi, A. Roux, M. Artico, O. Befani, T. Meninno, E. Agostinelli, P. Palmegiani, P. Turini, R. Cirilli, R. Ferretti, B. Gallinella, and F.L. Torre, *Design, synthesis, and biological activities of pyrrolylethanoneamine derivatives, a novel class of monoamine oxidases inhibitors*, J. Med. Chem. 48 (2005), pp. 4220–4223.
- [10] G.L. Regina, R. Silvestri, M. Artico, A. Lavecchia, E. Novellino, O. Befani, P. Turini, and E. Agostinelli, *New pyrrole inhibitors of monoamine oxidase: Synthesis, biological evaluation, and structural determinants of MAO-A and MAO-B selectivity*, J. Med. Chem. 50 (2007), pp. 922–931.
- [11] J.A. Morón, V. Pérez, M. Pastó, J.M. Lizcano, and M. Unzeta, *FA-70, a novel selective and irreversible monoamine oxidase-A inhibitor: effect on monoamine metabolism in mouse cerebral cortex*, J. Pharmacol. Expt. Therapeutics 292 (2000), pp. 788–794.
- [12] F. Chimenti, A. Bolasco, F. Manna, D. Secci, P. Chimenti, A. Granese, O. Befani, P. Turini, R. Cirilli, F. La Torre, S. Alcaro, F. Ortuso, and T. Langer, *Synthesis, biological evaluation and 3D-QSAR of 1,3,5-trisubstituted-4,5-dihydro-(1H)-pyrazole derivatives as potent and highly selective monoamine oxidase A inhibitors*, Curr. Med. Chem. 13 (2006), pp. 1411–1428.
- [13] A. Gallardo-Godoy, A. Fierro, T.H. McLean, M. Castillo, B.K. Cassels, M. Reyes-Parada, and D.E. Nichols, *Sulfur-substituted α -alkyl phenethylamines as selective and reversible MAO-A inhibitors: biological activities. CoMFA analysis, and active site modeling*, J. Med. Chem. 48 (2005), pp. 2407–2419.